TRAPPC6B biallelic variants cause a neurodevelopmental disorder with TRAPP II and trafficking disruptions

Hashem Almousa,[1,†] Sara A. Lewis,[2,3,†] Somayeh Bakhtiari,[2,3] Sandra Hinz Nordlie,[2,3] Alex Pagnozzi,[4] Helen Magee,[2,3] Stephanie Efthymiou,[5] Jennifer A. Heim,[2] Patricia Cornejo,[6,7,8] Maha S. Zaki,[9,10] Najwa Anwar,[11] Shazia Maqbool,[11] Fatima Rahman,[11] Derek E. Neilson,[12] Anusha Vemuri,[13] Sheng Chih Jin,[14] Xiao-Ru Yang,[15] Abolfazl Heidari,[16] Koen van Gassen,[17] Aurélien Trimouille,[18] Christel Thauvin-Robinet,[19,20,21] James Liu,[2,3] Ange-Line Bruel,[20,21] Hoda Tomoum,[22] Mennatallah O. Shata,[22] Mais O. Hashem,[23] Mehran Beiraghi Toosi,[24,25] Ehsan Ghayoor Karimiani,[26] Gözde Yeşil,[27] Lokesh Lingappa,[28] Debangana Baruah,[28] Farnoosh Ebrahimzadeh,[29] Julien Van-Gils,[17] Laurence Faivre,[19] Mina Zamani,[30,31] Hamid Galehdari,[30] Saeid Sadeghian,[32] Gholamreza Shariati,[31,33] Rahema Mohammad,[5] Jasper van der Smagt,[17] Alya Qari,[34] John B. Vincent,[35] A. Micheil Innes,[15] Ali Dursun,[36] R. Köksal Özgül,[36] Halil Tuna Akar,[36] Kaya Bilguvar,[37,38] Cyril Mignot,[39,40] Boris Keren,[39] Claudia Raveli,[41] Lydie Burglen,[42] Alexandra Afenjar,[42] Laura Donker Kaat,[43] Marjon van Slegtenhorst,[43] Fowzan Alkuraya,[23] Henry Houlden,[5] Sergio Padilla-Lopez,[2,3] Reza Maroofian,[5,‡] Michael Sacher[1,44,‡] and Michael C. Kruer[2,3,‡]

[†,‡]**These authors contributed equally to this work.**

Abstract

Highly conserved transport protein particle (TRAPP) complexes regulate subcellular trafficking pathways. Accurate protein trafficking has been increasingly recognized to be critically important for normal development, particularly in the nervous system. Variants in most TRAPP complex subunits have been found to lead to neurodevelopmental disorders with diverse but overlapping phenotypes. We expand on limited prior reports on *TRAPPC6B* with detailed clinical and neuroradiologic assessments, and studies on mechanisms of disease, and new types of variants.

We describe 29 additional patients from 18 independent families with biallelic variants in *TRAPPC6B*. We identified 7 homozygous nonsense (n=12 patients) and 8 canonical splice-site variants (n=17 patients). In addition, we identified one patient with compound heterozygous

splice-site/missense variants with a milder phenotype and one patient with homozygous missense variants.

Patients displayed non-progressive microcephaly, global developmental delay/intellectual disability, epilepsy, and absent expressive language. Movement disorders including stereotypies, spasticity, and dystonia were also observed. Brain imaging revealed reductions in cortex, cerebellum, and corpus callosum size with frequent white matter hyperintensity. Volumetric measurements indicated globally diminished volume rather than specific regional losses.

We identified a reduced rate of trafficking into the Golgi apparatus and Golgi fragmentation in patient-derived fibroblasts that was rescued by wild type TRAPPC6B. Molecular studies revealed a weakened interaction between mutant TRAPPC6B (c.454C>T, p.Q152*) and its TRAPP binding partner TRAPPC3. Patient-derived fibroblasts from the TRAPPC6B (c.454C>T, p.Q152*) variant displayed reduced levels of TRAPPC6B as well as other TRAPP II complex-specific members (TRAPPC9 and TRAPPC10). Interestingly, the levels of the TRAPPC6B homologue TRAPPC6A were found to be elevated. Moreover, co-immunoprecipitation experiments showed that TRAPPC6A co-precipitates equally with TRAPP II and TRAPP III, while TRAPPC6B co-precipitates significantly more with TRAPP II, suggesting enrichment of the protein in the TRAPP II complex. This implies that variants in *TRAPPC6B* may preferentially affect TRAPP II functions compared to TRAPP III functions. Finally, we assessed phenotypes in a *Drosophila TRAPPC6B*-deficiency model. Neuronal TRAPPC6B knockdown impaired locomotion and led to wing posture defects, supporting a role for TRAPPC6B in neuromotor function.

Our findings confirm the association of damaging biallelic *TRAPPC6B* variants with microcephaly, intellectual disability, language impairments, and epilepsy. A subset of patients also exhibited dystonia and/or spasticity with impaired ambulation. These features overlap with disorders arising from pathogenic variants in other TRAPP subunits, particularly components of the TRAPP II complex. These findings suggest that TRAPPC6B is essential for brain development and function, and TRAPP II complex activity may be particularly relevant for mediating this function.

Author affiliations:

1 Concordia University Department of Biology, Montreal, Quebec, H4B1R6, Canada

2 Barrow Neurological Institute, Phoenix Children's Hospital, Phoenix, AZ, 85016, USA

3 Departments of Child Health, Cellular and Molecular Medicine, Genetics, and Neurology, University of Arizona College of Medicine - Phoenix, Phoenix, AZ, 85004, USA

4 CSIRO Health and Biosecurity, The Australian e-Health Research Centre, Brisbane, 4029, Australia

5 Department of Neuromuscular Disorders, UCL Queen Square Institute of Neurology, London, WC1N 3BG, UK

6 Pediatric Neuroradiology Division, Pediatric Radiology, Barrow Neurological Institute, Phoenix Children's Hospital, Phoenix, AZ, 85016, USA

7 University of Arizona College of Medicine, Phoenix, AZ, 85004, USA

8 Mayo Clinic, Scottsdale, AZ, 85259, USA

9 Clinical Genetics Department, Human Genetics and Genome Research Division, National Research Centre, Cairo, 12622, Egypt

10 Genetics Department, Armed Forces College of Medicine (AFCM), Cairo, 4460015, Egypt.

11 Department of Developmental-Behavioural Paediatrics, The Children's Hospital and Institute of Child Health, Lahore, 54000, Pakistan.

12 Genetics and Metabolism, Phoenix Children's Hospital, 85016, Phoenix, AZ, USA

13 Department of Pathology, University of Chicago, Chicago, IL, 60637, USA

14 Department of Genetics, Washington University, St. Louis, MO, 63110, USA

15 Department of Medical Genetics and Alberta Children's Hospital Research Institute, Cumming School of Medicine, University of Calgary, S.W. Calgary, AB, T2N 4N1, Canada

16 Reference Laboratory of Qazvin Medical University, Qazvin, 34148-33245, Iran

17 Division of Laboratories, Pharmacy and Biomedical Genetics, Section of Clinical Genetics, University Medical Center Utrecht (UMCU), Utrecht, 3584 CX, Netherlands

18 Laboratoire de Génétique Moléculaire, Service de Génétique Médicale, CHU Bordeaux - Hôpital Pellegrin, Place Amélie Raba Léon, Bordeaux, 33000, France

19 Department of Genetics and Reference Center for Development disorders and intellectual disabilities, FHU TRANSLAD, CHU Dijon Bourgogne, Dijon, 21000, France

20 Unité Fontctionnelle d'Innovation diagnostiques des maladies rares, FHU TRANSLAD, CHU Dijon Bourgogne, Dijon, 21000, France.

21 INSERM-Université de Bourgogne UMR1231 GAD "Génétique des Anomalies du Développement", Dijon, 21078, France

22 Department of Pediatrics, Ain Shams University, Cairo, 11516, Egypt

23 Department of Translational Genomics, Center for Genomic Medicine, King Faisal Specialist Hospital and Research Centre, Riyadh, 11211, Saudi Arabia

24 Pediatric Neurology Department, Ghaem hospital, Mashhad University of Medical Sciences, Mashhad, 13944-91388, Iran

25 Neuroscience Research Center, Mashhad University of Medical Science, Mashhad, 13944-91388, Iran

26 Molecular and Clinical Sciences Institute, St. George's, University of London, Cranmer Terrace, London, SW17 0RE, UK

27 Istanbul University, Istanbul Medical Faculty Department of Medical Genetics, Istanbul, 34452, Turkey

28 Rainbow Children Hospital, Hyderabad, 500034, India

29 Department of Internal Medicine, Mashhad University of Medical Sciences, Mashhad, 13944-91388, lran

30 Department of Biology, Faculty of Science, Shahid Chamran University of Ahvaz, Ahvaz, 6135783151, Iran

31 Narges Medical Genetics and Prenatal Diagnosis Laboratory, Kianpars, Ahvaz, 6155889467, Iran

32 Department of Pediatric Neurology, Golestan Medical, Educational, and Research Center, Ahvaz Jundishapur University of Medical Sciences, Ahvaz, 6135733118, Iran

33 Department of Medical Genetics, Faculty of Medicine, Ahvaz Jundishapur University of Medical Sciences, Ahvaz, Iran

34 Medical Genomics Department, Center for Genomic Medicine, King Faisal Specialist Hospital and Research Center, Riyadh, 11564, Saudi Arabia.

35 Molecular Neuropsychiatry & Development (MiND) Lab, Campbell Family Mental Health Research Institute, Centre for Addiction and Mental Health, Toronto, ON, M6J 1H4, Canada

36 Hacettepe University, Faculty of Medicine&Institute of Child Health, Department of Pediatric Metabolism, Ankara, 06800, Turkey

37 Department of Medical Genetics, Acibadem Mehmet Ali Aydinlar University, Istanbul, 34752, Turkey

38 Department of Neurosurgery and Genetics, Yale University School of Medicine, New Haven, CT, 06520, USA

39 APHP Sorbonne Université, Département de Génétique, Hôpital Trousseau & Groupe Hospitalier Pitié-Salpêtrière, Paris, 75013, France

40 Centre de Référence Déficiences Intellectuelles de Causes Rares, Paris, 75012, France

41 APHP Sorbonne Université, Service de Neuropédiatrie, Hôpital Trousseau, Paris, 75012, France

42 Centre de référence des malformations et maladies congénitales du cervelet, Département de Génétique, APHP. Sorbonne Université, Hôpital Trousseau, 75012, Paris, France

43 Department of Clinical Genetics, Erasmus Medical Center, Rotterdam, 3000 CA, The Netherlands.

44 McGill University Department of Anatomy and Cell Biology, Montreal, Quebec, H3A0C7, Canada

Correspondence to: Associate Professor Michael Kruer

Departments of Child Health, Neurology, and Cellular & Molecular Medicine and Program in Genetics

University of Arizona College of Medicine – Phoenix

Arizona Biomedical Collaborative Building – 1

Phoenix, AZ 85004

E-mail: kruerm@arizona.edu

Running title: TRAPPC6B linked to neurodevelopment

Keywords: TRAPPC6B, NEDMEBA, TRAPPopathy, TRAPP-II complex, ER-golgi trafficking, Trs33

Introduction

Trafficking protein particle (TRAPP) complexes regulate vesicle trafficking via guanine nucleotide exchange factor (GEF) activity of Rab GTPases [1] and localization to compartments such as the Golgi apparatus [2]. Two TRAPP complexes have been identified in mammals called TRAPP II and TRAPP III. While both complexes activate Rab1 in vitro [2], TRAPP II additionally activates Rab11 [2,3], a GTPase that also functions in ciliogenesis [4]. TRAPP II proteins have also been implicated in ciliogenesis [5]. On the other hand, TRAPP III has been implicated in early secretory pathway traffic and autophagy [6,7]. Knockdowns and mutations in both TRAPP II- and III-specific proteins have been shown to affect trafficking into and through the Golgi as well as affecting Golgi morphology [8]. TRAPP-mediated trafficking is crucial for brain development and function, as variants in multiple TRAPP subunits lead to overlapping neurodevelopmental disorders, with movement disorders, intellectual disability (ID), epilepsy, and neuromuscular features (**Table 1**) [8].

Both TRAPP complexes are built upon a common catalytic core of proteins that include TRAPPC1, TRAPPC2, TRAPPC2L, TRAPPC3, TRAPPC4, TRAPPC5 and TRAPPC6. For the TRAPP II complex, TRAPPC9 and TRAPPC10 are linked to the core while the TRAPP III complex contains the core with TRAPPC8, TRAPPC11 and TRAPPC12 [6,9,10]. Two genes

encoding the core TRAPPC6 protein have been reported in humans called *TRAPPC6A* and *TRAPPC6B* [11]. *D.melanogaster* and *S.cerevisiae* have a single gene encoding this subunit, *Trs33*. It has been assumed that TRAPPC6A and TRAPPC6B could incorporate into either TRAPP II or TRAPP III complex, as both proteins are capable of forming a heterodimer in complex with TRAPPC3 *in vitro* [11-13].

A homozygous nonsense variant in *TRAPPC6B* was recently described in an Iranian family in association with intellectual disability [14] and a homozygous splice-site founder mutation was found in three Egyptian families in association with microcephaly, intellectual disability, autism, epilepsy, dystonia and reduced brain volume [15]. A fifth family was then reported [16]. In this report, we describe 29 individuals from 18 unrelated families with biallelic variants in *TRAPPC6B* manifesting microcephaly, epilepsy, and intellectual disability with phenotypic expansion to include spasticity. We examine variant impact on TRAPPC6B and TRAPP II- versus TRAPP III-specific protein levels, anterograde protein trafficking, and Golgi apparatus morphology in patient fibroblasts. Finally, we tested whether *TRAPPC6B* can regulate neuromotor function using *Drosophila* locomotor and wing posture assays. Together, the findings expand the *TRAPPC6B*-associated clinical and neuroradiologic phenotype and demonstrate patient variants disrupt TRAPPC6B and TRAPP II protein levels, trafficking, and Golgi morphology. We further find that TRAPPC6B preferentially associates with TRAPP II complex members, which support the observation that TRAPPC6B clinical phenotypes more closely align with TRAPP II complex disorders.

Materials and methods

Patient recruitment, sequencing and variant calling: All human subject studies were performed in accordance with the ethical standards of the responsible committee on human experimentation according to institutional and national standards. Proper informed consent was obtained for all participants. Clinical phenotypes (**Supplementary Clinical Summaries**) were abstracted from written records, supplemented by review of available neuroimaging, facial photographs, and laboratory and clinical electrophysiologic data. Patient videos were reviewed by pediatric movement disorder neurologists (J.H. and M.C.K.). Phenograms were created using

R (4.1.0). Patients with data not available for a category were not included in that category's calculations. TRAPP disease gene summary was created from OMIM.org, accessed August 2022. Sequencing details and filtering criteria used for each case are provided in the **Supplementary Methods**.

MRI analysis, processing and volumetric quantification: Neuroimaging findings were reviewed and summarized by a board-certified neuroradiologist (P.C.). Several image processing steps were then performed on the T1-weighted brain MRIs [17], including registration to the Colin 27 Average Brain Atlas, correcting image bias using the N4 algorithm, followed by intensity normalisation and image de-noising, using anisotropic diffusion. Skull stripping was performed using an in-house algorithm developed in Python. In this approach, intradural CSF was identified using thresholding and morphological operations, following which the lateral ventricles were isolated based on their spatial location, allowing the volume of the lateral ventricles (in mL) to be extracted. Cerebral brain tissues (grey matter, white matter) were then isolated based on their MR intensities using the Expectation Maximization (EM)/Markov Random Field (MRF) approach. From the cortical grey matter segmentation, three measures of cortical shape were performed (cortical thickness, curvature and sulcal depth) to quantify shape abnormalities. Measures were converted to a z-score from healthy cortical shape measures measured from the corresponding cortical region compared to the Child Mind Institute Healthy Brain Network cohort of 564 typically developing children (TDC) (Equation 1), based on cortical regions from the Automated Anatomical Labelling (AAL) atlas.

$$(Eqn\ 1)\ z-score_{subject} = \frac{(x_{subject} - \mu_{TDC})}{\sigma_{TDC}}$$

MRI statistical analysis: Six participants passed the quality checks for initial MRI data quality and processed segmentations (Families 3,4,6,10). For each participant, z-scores of grey matter volume, white matter volume, ventricle asymmetry (Equation 2), were extracted.

$$(Eqn\ 2)\ Ventricle\ asymmetry = \frac{(vol_{left} - vol_{right})}{(vol_{left} + vol_{right})}$$

Yeast Two Hybrid Assay: *TRAPP* open reading frames were cloned into pGADT7 and pGBKT7 plasmids (Clontech, USA). Standard yeast methods were used for transformation of the pGADT7 and pGBKT7 constructs into AH109 and Y187 yeast strains, respectively. Diploid cells were produced by mating on solid YPD media and then selected for on solid synthetic complete (SC) media lacking leucine and tryptophan (DDO). Single colonies of each diploid were then cultured in liquid DDO and then spotted on either DDO or on SC media lacking leucine, tryptophan and histidine (TDO) to assess for interactions. Plates were grown at 30°C for 72 hours.

Membrane Trafficking Assay: The retention using selective hooks (RUSH) assay was performed as described in Boncompain et al., 2012. Briefly, fibroblasts grown in Dulbecco's modified eagle medium (DMEM) supplemented with 10% fetal bovine serum were transfected by electroporation with the Golgi-resident enzyme sialyl transferase-GFP (ST-GFP) fused to streptavidin binding protein. The plasmid also expressed KDEL-tagged streptavidin for endoplasmic reticulum (ER) retention. For the rescue experiments, fibroblasts were co-transfected with ST-GFP and TRAPPC6B-RFP. 24 hours after transfection, biotin was added to a final concentration of 60 μM to release the reporter from the ER hook. Live cells were imaged by florescence microscopy every 2 minutes for 60 minutes using a Nikon Livescan sweptfield confocal microscope with a 40X objective lens (NA 0.95). Integrated fluorescence intensity at the Golgi region and from whole cell was measured every 2 minutes using ImageJ v1.53. The ratio between fluorescent intensities within the Golgi and whole cell was generated for each time point. The first time point corresponding to background was subtracted from all time points. These values were then plotted as the mean percentage of maximal intensity.

Golgi Morphology: Fibroblasts were cultured in DMEM supplemented with 10% fetal bovine serum. The cells were washed 2 times with phosphate buffered saline solution (PBS) then fixed with 4% paraformaldehyde (PFA) for 15 minutes at room temperature, quenched with 0.1 M glycine for 10 minutes and permeabilized with 0.1% Triton X-100 for 7 minutes. Blocking was performed in 5% normal goat serum in PBS for 45 minutes at room temperature. Primary antibodies were prepared in 5% normal goat serum and were added to the cells and incubated overnight at 4°C. Cells were washed 2 times for 5 minutes each with PBS. Secondary antibodies were diluted in 5% normal goat serum in PBS and incubated with the cells at room temperature

for one hour and then removed. Hoechst 33342 (Thermo Fisher Scientific) was diluted in PBS (1:2000) and added to stain the nucleus for 2 minutes followed by 2 washes with PBS wash for 10 minutes each. The coverslips were then mounted with Prolong Gold Anti Fade. Images were acquired on an Olympus FV10i confocal laser scanning microscope fitted with a 60X objective, NA 1.35. The number of Golgi fragments per cell were quantified using Imaris software c.9.8.0 (Bitplane, Concord, MA). Golgi structures were identified from the mannosidase II channel using the following surface parameters; surface details = 0.22µm and thresholding with a background subtraction of the depicted Golgi spherical structures that have diameter smaller than 0.55 µm in size. Statistical analyses were carried out using one-way ANOVA corrected for Tukey's multiple comparisons using GraphPad Prism 6.01. A p-value of 0.05 was considered to be statistically significant.

Immunoblotting: Fibroblasts were washed twice with PBS and lysed in a solution containing 50mM Tris pH 7.2, 150 mM NaCl, 0.5 mM EDTA, 1 mM DTT, 1% Triton X-100 and protease inhibitor cocktail (EDTA-free; Roche). The lysate was clarified at 13000×g for 30 minutes at 4°C. A total of 30-40 µg of whole cell lysate was loaded and fractionated in either 8% or 15% SDS-polyacrylamide gels (SDS-PAGE). The gels were transferred to nitrocellulose membranes and blocked with 5% skim milk powder in PBS with 0.1% Tween (PBS-T) for 1 hour. Primary antibodies were incubated in PBS-T overnight at 4°C, washed 3 times with PBS-T for 5 minutes each, and secondary antibodies were incubated for 1 hour at room temperature. Membranes were then washed 3 times with PBS-T for 5 minutes each and incubated with Pierce ECL western blot substrate (Thermo Fisher Scientific) and detected using an Amersham Imager 600 (GE Healthcare).

Immunoprecipitation: HeLa cells were seeded in 10cm dishes 24 hours prior to co-transfecting cells with 5µg of DNA expressing either TRAPPC6A-V5/TRAPPC10-FLAG, TRAPPC6A-V5/TRAPPC11-FLAG, TRAPPC6B-V5/TRAPPC10-FLAG, or TRAPPC6B-V5/TRAPPC11-FLAG using Jet Prime (Polyplus). 48 hours after transfection cells were washed twice with ice cold PBS and lysed in a solution containing 50mM Tris pH 7.2, 150 mM NaCl, 0.5 mM EDTA, 1 mM DTT, 1% Triton X-100 and protease inhibitor cocktail (EDTA-free; Roche). The lysate was clarified at 13000×g for 30 minutes at 4°C. A total of 500µg of lysate was incubated with 20µl (10µl bead volume) anti-Flag M2 affinity beads (Sigma Aldrich) in IP-buffer (50mM Tris

pH 7.2, 150 mM NaCl, 0.5 mM EDTA, 0.1% Triton X-100 and protease inhibitor cocktail) for 3 hours at 4°C on an orbital shaker. The beads were collected by centrifugation at 5000 rpm for 30 seconds at 4°C and washed 2 times with IP-buffer and 2 times with IP-buffer without Triton X-100. The beads were resuspended in 20µL of 2×Laemmli sample buffer containing β-mercaptoethanol and heated at 95°C for 5 minutes to dissociate the immune complexes. The beads were pelleted by centrifugation and SDS-PAGE for protein from input (whole-cell extracts) and immunoprecipitated proteins was performed as described above.

Molecular Biology Techniques: Standard molecular biological techniques were used to generate FLAG-tagged, RFP-tagged and V5 tagged constructs. TRAPPC6B variants were generated by site-directed mutagenesis.

Antibodies: Antibodies used in this study were: anti-TRAPPC2L (1:1000 mouse monoclonal, Santa Cruz sc-377322), anti-TRAPPC3 (1:1000 rabbit polyclonal,[18]), anti-TRAPPC6A (1:500 mouse monoclonal, Santa Cruz sc-376032), anti-TRAPPC6B (1:1000 rabbit polyclonal, ABclonal A15561), anti-TRAPPC8 (1:1000 rabbit polyclonal, Abcam ab122692), anti-TRAPPC9 (1:2000 rabbit polyclonal, LS Bio LS-C750497), anti-TRAPPC10 (1:500 mouse monoclonal, Santa Cruz sc-101259), anti-TRAPPC12 (1:1000 rabbit polyclonal, [18]), anti-FLAG (1:5000 mouse monoclonal, Sigma F1804), anti-α-Tubulin (1:5000 mouse monoclonal, Sigma T6199), anti-RFP (1:500 mouse monoclonal, Rockland 200-301-379S), anti-mannosidase II (1:200 kind gift from Dr Kelley Moreman), anti V5 (1:1000 rabbit monoclonal, Cell Signaling 13202).

Fly rearing and genetics: *Drosophila* were reared on a standard cornmeal, yeast, sucrose food from the BIO5 media facility, University of Arizona. Stocks for experiments were reared at 25°C, 60-80% relative humidity with 12:12 light/dark cycle. Crosses for controls and mutants and animals selected for locomotor assay were maintained at an elevated temperature of 28.5°C. Fly stocks were obtained from the Bloomington Drosophila Stock Center (NIH P40OD018537). Crosses were performed with w^{1118} for heterozygous studies of genetic controls. P[TRiP.HMJ21139]attP40 was used for expression of UAS-Trs33-RNAi [19]. Pan-neuronal Gal-4 driver (ELAV, CG4262) was used to direct RNAi expression to post-mitotic neurons during development and throughout adulthood.

Locomotor assays: Naïve, unmated flies collected as pharate adults and controlled for humidity, temperature, and time of day (30% RH, 24°C, 0900-1100) were used. Flies at 14 days post-eclosion were adapted to room conditions for 1 hour before assaying in groups of 3-20 in coded vials by blinded experimenters [20]. Distance was determined from still images from video at 3 seconds post-tapping using ImageJ measured distance function from the middle of the fly to the bottom of the vial and averaged between flies for each trial. Graphs and t-test statistic calculations were performed in R (4.1.0). For box and whisker plots, box indicates 75th and 25th percentile with median line; whiskers indicate range of data.

Erect wing scoring: Each video was manually assessed for flies with erect wing phenotype defined as wings held upright and away from the body [21]. The wing must have been held erect during the majority of the video, and upright wing postures limited to before flight or during grooming were excluded. Statistics were determined both as a 3-way and pairwise against both control genotypes using Chi-squared analysis in R (4.1.0).

Results

Through Genematcher, we identified 18 families with biallelic variants in *TRAPPC6B* from international collaborators. In our cohort, 27/29 individuals segregated loss of function (LoF) (nonsense and splice-site) homozygous variants, with one individual carrying compound heterozygous splice-site/missense variants and one individual carrying homozygous missense variants. The M:F ratio was 1.6:1 and average age of diagnosis was 7.5 years (range 14 months to 35 years). Affected families were from 11 countries (Iran, Morocco, Pakistan, Tunisia, France, Mali, Gambia, Egypt, Saudi Arabia, Turkey, India) and frequently included multiple affected individuals (**Supplementary Fig. 1**). Homozygous variants including 7 homozygous nonsense (n= 12 individuals), 8 canonical splice-site variants (n=17 individuals), and 1 missense variant (n=1 individuals) were identified using whole exome sequencing (WES). Variant information is provided in **Supplementary Table 1**. Additional sequencing information is provided in **Supplementary Methods**.

We conducted detailed clinical and neuroradiologic assessments. Frequency of clinical features are summarized in **Table 2** and **Fig. 1A** with full descriptions in the **Supplementary Clinical Summaries**. We noted a constellation of cognitive and motor features partially overlapping a prior report of individuals with *TRAPPC6B* variants (Marin-Valencia et al., 2018). Consistent with prior reports, we found complex neurodevelopmental features including intellectual disability, expressive language defects, autism, seizures or epilepsy, and neurobehavioral features such as aggression and self-injury in some patients (**Fig. 1A**). Many patients also exhibited difficulty with walking and some also had issues sitting. Stereotyped movements were evident in most individuals, with dystonia, spasticity, and contractures, at lower frequency. On examination, knee-jerk reflexes were often increased, although they were absent in one patient. Reduced muscle bulk was occasionally observed in the most impaired patients (GMFCS 4-5). Microcephaly was a notable feature in this cohort, with some patients as severe as <-6.5 SD. This microcephaly does not appear to be progressive based on serial clinical assessments. Dysmorphic features include a variety of inconsistent facial features, tapered fingers, and arachnodactyly (**Fig. 1B-N**). MRI was assessed for 16 individuals (**Fig. 2**) and identified reductions in cortex and cerebellum with increased ventricle size. Foreshortening or thinning of corpus callosum and white matter increased intensity or volume loss were consistent imaging features. Volumetric measures of MRI compared to age-matched large populations [17] did not identify a specific region driving the observed microcephaly (**Fig. 2N**). Of note, the individuals with missense variants (patients 7 and 29) exhibited similar phenotypes, suggesting that missense variants could potentially impair protein function and disrupt nervous system development.

TRAPPC6B p.Q152* impairs TRAPPC3 binding and diminishes protein expression for TRAPPC6B and TRAPP II complex members

Given that our previous work suggested that the carboxy-terminus of TRAPPC6A interacts with adaptor subunit TRAPPC2L and both TRAPPC6A and TRAPPC6B interact with TRAPPC2L and TRAPPC3 [22], we examined interactions between TRAPPC6B and both TRAPPC2L and TRAPPC3. While an interaction between both TRAPPC2L and TRAPPC3 was seen for the wild type TRAPPC6B irrespective of the vectors used, only the TRAPPC3

interaction was affected by the p.Q152* allele from affected individuals in family 15 (**Fig. 3A and 3B**).

This result suggests that the carboxy-terminus of TRAPPC6B is important for its interaction with TRAPPC3 and that this interaction is diminished in TRAPPC6B p.Q152*. Since the TRAPPC3-TRAPPC6B heterodimer is important for the assembly of the TRAPP complexes, it is not unreasonable to expect that TRAPPC6B variants will decrease the presence of subunits that rely on this heterodimer to associate with TRAPP complexes. Indeed, in p.Q152* fibroblasts, several TRAPP protein levels were decreased, with the strongest effect seen for the two TRAPP II-specific proteins TRAPPC10 and TRAPPC9 (**Fig. 3C**). There was a near complete absence of detectable amounts of TRAPPC6B, suggesting potential nonsense mediated decay or truncated protein instability (**Fig. 3C**). It is noteworthy that we consistently saw an increase in the levels of TRAPPC6A in the fibroblasts from the affected individuals, perhaps representing an attempted compensatory response.

TRAPP II complex members associate preferentially with TRAPPC6B

We next examined whether TRAPPC6B was preferentially associated with TRAPP II complexes. To perform this experiment, HeLa cells were mock transfected or co-transfected with TRAPPC6A-V5/TRAPPC10-FLAG, TRAPPC6A-V5/TRAPPC11-FLAG, TRAPPC6B-V5/TRAPPC10-FLAG, or TRAPPC6B-V5/TRAPPC11 and associated proteins were collected on beads harboring anti-FLAG IgG and probed for V5 and FLAG. TRAPPC11 transfections target TRAPP III while the TRAPPC10 transfections target TRAPP II.

Unlike TRAPPC6A, which equally co-precipitated with TRAPPC10 and TRAPPC11, TRAPPC6B was significantly more enriched with TRAPPC10 compared to TRAPPC11 (**Fig. 4A and 4B**). These results suggest that TRAPP II complexes are enriched in TRAPPC6B compared to TRAPP III.

Patient-derived fibroblasts have ER-Golgi trafficking defects and altered Golgi morphology

Previous studies have shown an anterograde trafficking defect for variants in most TRAPP-associated genes [8,22-24]. Therefore, we subjected fibroblasts derived from families 4 (c.149+2 T>A splice-site; patients 5 and 6) and 15 (p.Q152*; patients 23 and 24) to a membrane trafficking assay [25]. In all four cases, upon biotin-mediated release of an ER-retained protein there was a delay in transport to the Golgi compared to control (**Fig. 5A and 5B**). This was determined to be TRAPPC6B-related since transfection of RFP-tagged TRAPPC6B resulted in a noticeable rescue of this trafficking defect. Golgi fragmentation is also commonly seen in cells harboring TRAPP gene mutations as well as in cells with mutations in other membrane trafficking-related proteins [26]. When the fibroblasts from affected individuals were compared to control, a significant increase in Golgi fragmentation was seen (**Fig. 5C and 5D**). This increase was rescued to near wild type levels by transfection of wild type TRAPPC6B. Together, our functional studies suggest that variants in TRAPPC6B can disrupt ER to Golgi protein trafficking and lead to altered Golgi morphology.

Loss of neuronal TRAPPC6B impairs locomotion and wing posture in *Drosophila*

We examined whether TRAPPC6B could regulate neuromotor function in a *Drosophila* model. The *Drosophila* ortholog, Trs33, has excellent conservation with TRAPPC6B (DIOPT score=15/15) with 72% similarity and 54% identity (flyrnai.org). As Trs33 is an essential gene for development, we utilized an RNAi knockdown approach specifically in neurons under the ELAV-Gal4 driver. Neuronal expression of Trs33 shRNA decreased distance traveled in a locomotor assay compared to the heterozygous controls of the Gal4 and UAS lines alone (**Fig. 6A**). Additionally, an abnormality of wing posture was noted in 10.6% of these animals, suggesting defects in the innervation of the indirect flight muscles (**Fig. 6B**). Together, this suggests TRAPPC6B is crucial for motor function.

Discussion

Marin-Valencia et al. recently reported a founder *TRAPPC6B* homozygous splice-site variant segregating with disease in 3 Egyptian families and found that morpholino treatment against *Danio* TrappC6B led to reduced head size and increased spontaneous neuronal activity in zebrafish. We present here 29 individuals from 18 families with biallelic variants in *TRAPPC6B*. These individuals share a syndromic phenotype consisting of primary microcephaly, global

developmental delay/intellectual disability, stereotypies and impaired expressive language. Brain MRI findings include volume loss, thin corpus callosum, and white matter signal abnormalities. Variable features include epilepsy, spasticity/dystonia, and dysmorphic features. Our findings thus provide an independent validation for biallelic *TRAPPC6B* variants as a cause of a complex neurodevelopmental disorder and expand on the clinical features.

Notably, two individuals in our series harbored *TRAPPC6B* variants of unknown significance (patients 7 and 29). The individual with compound heterozygous splice and small deletion variants (patient 7) had a milder phenotype, gaining the ability to use limited expressive language, falling short of a formal diagnosis of microcephaly, and achieving independent walking by age 3. The homozygous missense variant (p.G124V) has a CADD score of 32, is absent from gnomAD, and classified as a VOUS in Varsome. This individual (patient 29) has clinical features that match the remaining cohort, including microcephaly, spasticity, epilepsy, and a thin corpus callosum. However, we were not able to conduct functional studies on this variant. This suggests that missense variants can contribute to a *TRAPPC6B* genetic disorder, with similar but potentially milder manifestations, but further studies are needed. The remaining 27 individuals in the present cohort and those reported by Marin-Valencia all had homozygous splice-site and early stop variants. We confirmed diminished protein expression in a family with a homozygous early stop variant (p.Q152*), consistent with a loss of function variant that may manifest with decreased protein abundance or the loss of an as-yet unidentified motif in the carboxy-terminus important for subcellular localization or protein-protein interactions. One limitation of this work is the fact that we only tested the effect of this particular variant on TRAPPC6B levels.

Our biochemical studies suggest that variants in TRAPPC6B such as p.Q152* likely impair TRAPP II complex stability by a weakened interaction with TRAPPC3 and decreasing protein expression for TRAPPC6B and TRAPP II complex members. TRAPPC6B appears to preferentially associate with TRAPP II compared to TRAPP III. It is interesting that TRAPPC6A levels increase in the absence of TRAPPC6B as seen in affected individuals of family 15. It is possible that TRAPPC6A can partially compensate for the loss of TRAPPC6B. This would be consistent with the studies of TRAPP guanine nucleotide exchange factor (GEF) activity towards Rab for recombinant *Drosophila* and human complexes [3,27]. In *Drosophila*, only a single

(TRAPPC6B) homologue is found, while humans have both TRAPPC6A and TRAPPC6B. Therefore, *Drosophila* TRAPP complexes do not distinguish between the two TRAPPC6 human orthologues and TRAPP III is functional with TRAPPC6B. In the human recombinant complexes, TRAPPC6A was used for assembling both TRAPP II and III, and both complexes were functional [3,27]. It remains possible that had TRAPPC6B been used in the recombinant TRAPP II complex, stronger or additional GEF activity would have been seen. Nevertheless, our present study suggests a bias for TRAPPC6B in TRAPP II and implies the cell has a mechanism to distinguish and incorporate specific TRAPPC6 orthologues into specific TRAPP complexes. It is presently unclear how this would be accomplished.

Disruption of TRAPP II stability has been shown previously to affect anterograde trafficking (Rawlins et al., 2022). Biallelic variants of *TRAPPC6B* show similar cellular features, such as an ER- to -Golgi trafficking defect and altered Golgi morphology.

We found that neuronal loss of TRAPPC6B in a *Drosophila* model impaired locomotion and wing posture. The erect wing phenotype has been linked to impaired synaptic growth [28] and disrupted central nervous system commissures and longitudinal tracts innervating the indirect flight muscles which regulate wing posture [29]. Knocking down Trs33 in *Drosophila* with the Mef2 muscle and neuron expressing Gal4-driver was reported to impair flight ability, but without obvious changes to the flight muscles, myofibrils, or sarcomeres themselves [30]. Together with our ELAV-mediated neuronal knockdown, this suggests a neuronal origin for the previously reported flight muscle weakness that has similarities to the postural/locomotor impairments in *TRAPPC6B*-affected individuals.

TRAPPC6B-associated phenotypes overlap substantially with variants in genes encoding other TRAPP subunits. These phenotypes include intellectual disability, movement disorders, white matter involvement, cerebellar volume loss, microcephaly, and muscle involvement (**Table 1**) [8]. Many TRAPP-related disorders, particularly those affecting TRAPP III, identified a progressive loss of cerebral volume over time (**Table 1**). However, we did not find evidence that loss of *TRAPPC6B* function causes neurodegeneration. Treating clinicians did not note progressive microcephaly and available OFC measurements seem to start low at birth and maintain the same course. Consistent with the biochemical studies, we found *TRAPPC6B*

phenotypes overlapped more closely for genes exclusively localized to TRAPP II (*TRAPPC9* (#613192) and *TRAPPC10* (*602103)). In contrast, individuals with variants in genes exclusively encoding autophagy-associated TRAPP III components (*TRAPPC11* and *TRAPPC12*) are notably different from the *TRAPPC6B* patients. *TRAPPC11* variants lead to a complex neurodevelopmental disorder with muscular dystrophy and visual system impairments and individuals with *TRAPPC12* display a progressive encephalopathy. This supports the conclusion that *TRAPPC6B* is important for TRAPP II complex function with impairments resulting in a distinct and recognizable TRAPPopathy. A major challenge in understanding the neurological disorder linked to TRAPPII variants is the consequence of trafficking defects on neuronal function. We identified a potential defect in neuronal innervation in the fly model, however we were unable to investigate further due to the lack of human neuronal cells. Cellular reprograming of patient fibroblasts into patient-derived induced pluripotent stem cells (iPSCs) that can be induced to differentiate into specific neuronal cells can overcome this limitation and provide better insight into the etiology of NDDs associated with TRAPPII variants.

Data availability

The authors confirm that the data supporting the findings of this study are available within the article and/or its supplementary material. Additional raw and/or de-identified data supporting the findings of this study are available from the corresponding authors upon reasonable request.

Acknowledgements

We are grateful to the patients and their families for involvement in these studies. We acknowledge Dr. Hossein Mozhdehipanah and Dr. Paulien A. Terhal for providing patient clinical information. We appreciate the assistance of Dr. Bob Argiropoulos and Nadine Gamache with fibroblast cultures.

Funding

Portions of this work were supported by a Cerebral Palsy Alliance Research Foundation Career Development Award to SB, and by the U.S. National Institutes of Health (1R01NS106298 and 1R01NS127108 to MCK).

Competing interests

The authors have no competing interests to report that could influence the conclusions of this manuscript.

Supplementary material

Supplementary material is available at *Brain* online.

References

1. Chin HF, Cai Y, Menon S, Ferro-Novick S, Reinisch KM, De La Cruz EM. Kinetic analysis of the guanine nucleotide exchange activity of TRAPP, a multimeric Ypt1p exchange factor. *J Mol Biol*. Jun 5 2009;389(2):275-88. doi:10.1016/j.jmb.2009.03.068

2. Riedel F, Galindo A, Muschalik N, Munro S. The two TRAPP complexes of metazoans have distinct roles and act on different Rab GTPases. *J Cell Biol*. Feb 5 2018;217(2):601-617. doi:10.1083/jcb.201705068

3. Jenkins ML, Harris NJ, Dalwadi U, *et al*. The substrate specificity of the human TRAPPII complex's Rab-guanine nucleotide exchange factor activity. *Commun Biol*. Dec 4 2020;3(1):735. doi:10.1038/s42003-020-01459-2

4. Knödler A, Feng S, Zhang J, *et al*. Coordination of Rab8 and Rab11 in primary ciliogenesis. *Proc Natl Acad Sci U S A*. Apr 6 2010;107(14):6346-51. doi:10.1073/pnas.1002401107

5. Westlake CJ, Baye LM, Nachury MV, *et al*. Primary cilia membrane assembly is initiated by Rab11 and transport protein particle II (TRAPPII) complex-dependent trafficking of Rabin8 to the centrosome. *Proc Natl Acad Sci U S A*. Feb 15 2011;108(7):2759-64. doi:10.1073/pnas.1018823108

6. Scrivens PJ, Noueihed B, Shahrzad N, Hul S, Brunet S, Sacher M. C4orf41 and TTC-15 are mammalian TRAPP components with a role at an early stage in ER-to-Golgi trafficking. *Mol Biol Cell*. Jun 15 2011;22(12):2083-93. doi:10.1091/mbc.E10-11-0873

7. Stanga D, Zhao Q, Milev MP, Saint-Dic D, Jimenez-Mallebrera C, Sacher M. TRAPPC11 functions in autophagy by recruiting ATG2B-WIPI4/WDR45 to preautophagosomal membranes. *Traffic*. May 2019;20(5):325-345. doi:10.1111/tra.12640

8. Sacher M, Shahrzad N, Kamel H, Milev MP. TRAPPopathies: An emerging set of disorders linked to variations in the genes encoding transport protein particle (TRAPP)-associated proteins. *Traffic*. Jan 2019;20(1):5-26. doi:10.1111/tra.12615

9. Bassik MC, Kampmann M, Lebbink RJ, *et al*. A systematic mammalian genetic interaction map reveals pathways underlying ricin susceptibility. *Cell*. Feb 14 2013;152(4):909-22. doi:10.1016/j.cell.2013.01.030

10. Scrivens PJ, Shahrzad N, Moores A, Morin A, Brunet S, Sacher M. TRAPPC2L is a novel, highly conserved TRAPP-interacting protein. *Traffic*. Jun 2009;10(6):724-36. doi:10.1111/j.1600-0854.2009.00906.x

11. Kümmel D, Müller JJ, Roske Y, Henke N, Heinemann U. Structure of the Bet3-Tpc6B core of TRAPP: two Tpc6 paralogs form trimeric complexes with Bet3 and Mum2. *J Mol Biol*. Aug 4 2006;361(1):22-32. doi:10.1016/j.jmb.2006.06.012

12. Tokarev AA, Taussig D, Sundaram G, *et al*. TRAPP II complex assembly requires Trs33 or Trs65. *Traffic*. Dec 2009;10(12):1831-44. doi:10.1111/j.1600-0854.2009.00988.x

13. Kümmel D, Oeckinghaus A, Wang C, Krappmann D, Heinemann U. Distinct isocomplexes of the TRAPP trafficking factor coexist inside human cells. *FEBS Lett*. Nov 12 2008;582(27):3729-33. doi:10.1016/j.febslet.2008.09.056

14. Harripaul R, Vasli N, Mikhailov A, *et al.* Mapping autosomal recessive intellectual disability: combined microarray and exome sequencing identifies 26 novel candidate genes in 192 consanguineous families. *Mol Psychiatry*. Apr 2018;23(4):973-984. doi:10.1038/mp.2017.60

15. Marin-Valencia I, Novarino G, Johansen A, *et al.* A homozygous founder mutation in TRAPPC6B associates with a neurodevelopmental disorder characterised by microcephaly, epilepsy and autistic features. *J Med Genet.* Jan 2018;55(1):48-54. doi:10.1136/jmedgenet-2017-104627

16. Nair P, El-Bazzal L, Mansour H, *et al.* Further Delineation of the TRAPPC6B Disorder: Report on a New Family and Review. *J Pediatr Genet.* Dec 2019;8(4):252-256. doi:10.1055/s-0039-1693664

17. Pagnozzi AM, Dowson N, Doecke J, *et al.* Identifying relevant biomarkers of brain injury from structural MRI: Validation using automated approaches in children with unilateral cerebral palsy. *PLoS One*. 2017;12(8):e0181605. doi:10.1371/journal.pone.0181605

18. Milev MP, Hasaj B, Saint-Dic D, Snounou S, Zhao Q, Sacher M. TRAMM/TrappC12 plays a role in chromosome congression, kinetochore stability, and CENP-E recruitment. *J Cell Biol.* Apr 27 2015;209(2):221-34. doi:10.1083/jcb.201501090

19. Ke H, Feng Z, Liu M, *et al.* Collagen secretion screening in Drosophila supports a common secretory machinery and multiple Rab requirements. *J Genet Genomics*. Jun 1 2018;doi:10.1016/j.jgg.2018.05.002

20. Kim M, Sandford E, Gatica D, *et al.* Mutation in ATG5 reduces autophagy and leads to ataxia with developmental delay. *eLife.* Jan 2016;5:e12245.

21. Fernandes C, Rao Y. Genome-wide screen for modifiers of Parkinson's disease genes in Drosophila. *Mol Brain*. Apr 19 2011;4:17. doi:10.1186/1756-6606-4-17

22. Al-Deri N, Okur V, Ahimaz P, *et al.* A novel homozygous variant in TRAPPC2L results in a neurodevelopmental disorder and disrupts TRAPP complex function. *J Med Genet*. Sep 2021;58(9):592-601. doi:10.1136/jmedgenet-2020-107016

23. Van Bergen NJ, Guo Y, Al-Deri N, *et al.* Deficiencies in vesicular transport mediated by TRAPPC4 are associated with severe syndromic intellectual disability. *Brain*. Jan 1 2020;143(1):112-130. doi:10.1093/brain/awz374

24. Rawlins LE, Almousa H, Khan S, *et al*. Biallelic variants in TRAPPC10 cause a microcephalic TRAPPopathy disorder in humans and mice. *PLoS Genet*. Mar 2022;18(3):e1010114. doi:10.1371/journal.pgen.1010114

25. Boncompain G, Divoux S, Gareil N, *et al*. Synchronization of secretory protein traffic in populations of cells. *Nat Methods*. Mar 11 2012;9(5):493-8. doi:10.1038/nmeth.1928

26. Makhoul C, Gosavi P, Gleeson PA. Golgi Dynamics: The Morphology of the Mammalian Golgi Apparatus in Health and Disease. *Front Cell Dev Biol*. 2019;7:112. doi:10.3389/fcell.2019.00112

27. Harris NJ, Jenkins ML, Dalwadi U, *et al*. Biochemical Insight into Novel Rab-GEF Activity of the Mammalian TRAPPIII Complex. *J Mol Biol*. Sep 3 2021;433(18):167145. doi:10.1016/j.jmb.2021.167145

28. Haussmann IU, White K, Soller M. Erect wing regulates synaptic growth in Drosophila by integration of multiple signaling pathways. *Genome Biol*. Apr 17 2008;9(4):R73. doi:10.1186/gb-2008-9-4-r73

29. DeSimone S, Coelho C, Roy S, VijayRaghavan K, White K. ERECT WING, the Drosophila member of a family of DNA binding proteins is required in imaginal myoblasts for flight muscle development. *Development*. Jan 1996;122(1):31-9. doi:10.1242/dev.122.1.31

30. Schnorrer F, Schönbauer C, Langer CC, *et al*. Systematic genetic analysis of muscle morphogenesis and function in Drosophila. *Nature*. Mar 11 2010;464(7286):287-91. doi:10.1038/nature08799

31. Milev MP, Graziano C, Karall D, et al. Bi-allelic mutations in TRAPPC2L result in a neurodevelopmental disorder and have an impact on RAB11 in fibroblasts. J Med Genet. Nov 2018;55(11):753-764. doi:10.1136/jmedgenet-2018-105441

32. Saad AK, Marafi D, Mitani T, et al. Biallelic in-frame deletion in TRAPPC4 in a family with developmental delay and cerebellar atrophy. Brain. Oct 1 2020;143(10):e83. doi:10.1093/brain/awaa256

33. Ghosh SG, Scala M, Beetz C, et al. A relatively common homozygous TRAPPC4 splicing variant is associated with an early-infantile neurodegenerative syndrome. Eur J Hum Genet. Feb 2021;29(2):271-279. doi:10.1038/s41431-020-00717-5

34. Mohamoud HS, Ahmed S, Jelani M, et al. A missense mutation in TRAPPC6A leads to build-up of the protein, in patients with a neurodevelopmental syndrome and dysmorphic features. Sci Rep. Feb 1 2018;8(1):2053. doi:10.1038/s41598-018-20658-w

35. Bodnar B, DeGruttola A, Zhu Y, et al. Emerging role of NIK/IKK2-binding protein (NIBP)/trafficking protein particle complex 9 (TRAPPC9) in nervous system diseases. Transl Res. Oct 2020;224:55-70. doi:10.1016/j.trsl.2020.05.001

36. Kakar N, Goebel I, Daud S, et al. A homozygous splice site mutation in TRAPPC9 causes intellectual disability and microcephaly. Eur J Med Genet. Dec 2012;55(12):727-31. doi:10.1016/j.ejmg.2012.08.010

37. Santos-Cortez RLP, Khan V, Khan FS, et al. Novel candidate genes and variants underlying autosomal recessive neurodevelopmental disorders with intellectual disability. Hum Genet. Sep 2018;137(9):735-752. doi:10.1007/s00439-018-1928-6

38. Wang X, Wu Y, Cui Y, Wang N, Folkersen L, Wang Y. Novel TRAPPC11 Mutations in a Chinese Pedigree of Limb Girdle Muscular Dystrophy. Case Rep Genet. 2018;2018:8090797. doi:10.1155/2018/8090797

39. Milev MP, Grout ME, Saint-Dic D, et al. Mutations in TRAPPC12 Manifest in Progressive Childhood Encephalopathy and Golgi Dysfunction. Am J Hum Genet. Aug 3 2017;101(2):291-299. doi:10.1016/j.ajhg.2017.07.006

Figure 1 Clinical features of patients with TRAPPC6B variants. A: Phenogram of frequency of phenotypic features for 29 new patients and 8 previously reported patients (**Supplementary Table 1**). ID/DD=intellectual disability/developmental disability). Fields with missing data were not included in calculations for that feature. Behavioral phenotypes include aggression, self-injury, anxiety, and hyperactivity. **B-N**: Photos of dysmorphic features. No unifying dysmorphic features were observed. **B-C:** Patient 1 (Family 1) has gingival hypertrophy and swan neck deformity of fingers, representing dystonia. Patient also exhibited spastic-dystonic quadriplegia with contractures in the elbow flexors and plantar flexors, temporal wasting, muscle atrophy, and curling of all her toes (not shown)**. C:** Patient 2 (Family 1) has synophrys, bitemporal narrowing, prominent cheekbones, a wide nasal root and bridge, and a papular lesion suspicious for an

occult encephalocele. Patient also exhibited spastic-dystonic quadripledia, brachycephaly, trigonocephaly, temporal wasting and muscle atrophy in his proximal limb muscle (not shown). **E:** Patient 5 (Family 4) has microcephaly, bitemporal narrowing, low anterior hairline, deep-set eyes, prominent ears, long nose with narrow nasal bridge, prognathia. **F:** Patient 6 (Family 4) has microcephaly, bitemporal narrowing strabismus, positional plagiocephaly, deep set eyes, broad nasal root and narrow nasal bridge, and widely spaced teeth**. G:** Patient 7 (Family 5) showing depressed nasal bridge, upturned nasal tip, and thin upper lip. Patient also exhibited bilateral clinodactyly, tapered fingers, and inverted nipples (not shown). **H-I:** Patient 10 (Family 8) has microcephaly, long face, arched eyebrows, wide spaced eyes, almond shaped eye, straight nasal bridge, broad nose, broad chin, and low set ears. Patient also exhibited arachnodactyly (not shown). **J-K:** Patient 17 (Family 11) has narrow nasal bridge, posteriorly rotated ears. **L:** Patient 18 (Family 11) has upslanting palpebral fissures, square nasal tip. **M-N:** Patient 19 (Family 12) has microcephaly, bulbous nasal tip, and creased earlobe.

Figure 2 Qualitative and quantitative analysis of the MRI images. A, C, E, G, I, K: Sagittal MRI T1 weighted midline images. **B, H:** Axial FLAIR images. **D, F, J, L:** Axial MRI T2 weighted images. **A-B:** Patient 3, Family 2: 13-year-old female. **A.** Small craniofacial ratio, thinning/foreshortening of the corpus callosum with greater involvement of the posterior fibers (red arrow). **B:** Patchy FLAIR signal hyperintensity in the bilateral periventricular white matter (arrows) extending to the centrum semiovale, peri Rolandic and peri atrial regions (not shown). **C-D:** Patient 5**,** Family 4: 13-year-old female. **C.** Small craniofacial ratio, diffuse thinning/foreshortening of the corpus callosum (red arrow), and brainstem and cerebellum volume loss (cyan arrow). **D:** Abnormal angulation of the posterior margins of the ventricles (arrows). **E-F:** Patient 6, Family 4: 9-year-old female. **E.** Small craniofacial ratio, thinning/foreshortening of the corpus callosum and posterior greater than anterior parenchymal loss (arrow). **F:** Diffuse parenchymal loss with preferential involvement of the posterior lobes, ex-vacuo dilatation and angulation of the ventricles (arrows). **G-H.** Patient 13, Family 10: 6-year-old male. **G.** Reduced FOD (frontal occipital diameter) diffuse thinning and foreshortening of the corpus callosum (arrow). **H.** Patchy FLAIR signal hyperintensity in peri atrial white matter associated with abnormal square shape of the posterior margins of the lateral ventricles (arrows). **I-J.** Patient 14, Family 10: 2-year-old female. **I.** Reduced FOD, diffuse thinning and

foreshortening of the corpus callosum (arrow). **J.** Increased T2 signal in peri atrial white matter associated with abnormal angulation of the posterior margins of the lateral ventricles (arrows). **K-L.** Patient 16, Family 10: 5-year-old female. **K.** Marginal FOD (red arrow) and inferior vermis hypoplasia (cyan arrow). **L.** No signal abnormalities present. **M.** Phenogram of MRI features for 16 new patients and 7 previously reported patients with MRI interpretation. Patient-specific details are provided in **Supplemental Table 1**. VM=ventriculomegaly. WMI=white matter hyperintensity or abnormalities. CC=corpus callosum. CB=cerebellum. CTX=cortex. **N.** Box and whisker plot of six structural measures quantified from brain MRI volumes of 6 patients, represented as Z scores, in comparison to an age-matched control cohort of typically developing children. The threshold for significance of -1 SD indicates reduced volume compared to the general population. Volume loss was identified in the cerebellum (CB), but there was no consistent reduction in other measurements. Ventricle asymmetry (Vent) measures laterality of ventricle expansion; no asymmetry was detected. Boxes represent 25th and 75th percentiles with median line; whiskers represent data range. GM=grey matter, DGM=deep grey matter, CB=cerebellum, WM=white matter, CC=corpus callosum, Vent=ventricle asymmetry.

Figure 3 TRAPPC6B variants affect the stability of TRAPP II. TRAPPC6B (wild type or the p.Q152* variant), were cloned into either pGADT7 (**A**) or pGBKT7 (**B**), TRAPPC2L and TRAPPC3 were cloned into either pGBKT7 (**A**) or pGADT7 (**B**) and transformed into haploid yeast cells. In some cases, an empty vector was used (indicated asΦ). The cells were mated, diploids selected and then spotted as serial dilutions on plates lacking leucine and tryptophan (DDO) or plates lacking leucine, tryptophan and histidine (TDO). **C.** Fibroblasts from control or affected individuals from family 15 (p.Q152*) were lysed and probed for the indicated TRAPP proteins or for tubulin as a loading control.

Figure 4 TRAPPC6B Preferentially Associates with the TRAPP II Complex. A. HeLa cells were either untransfected (NT) or co-transfected with TRAPPC6A-V5/TRAPPC10-FLAG, TRAPPC6A-V5/TRAPPC11-FLAG, TRAPPC6B-V5/TRAPPC10-FLAG, or TRAPPC6B-V5/TRAPPC11. After 48 hours the cells were lysed and treated with anti-FLAG IgG agarose beads. The eluates from the immunoprecipitation were probed for V5, FLAG and Tubulin. The

blot is representative of at least three biological replicates. Inputs represent 10% of the sample subjected to immunoprecipitation. **B.** Quantification of the ratio of V5 immunoprecipitated with FLAG from three different experiments. The integrated density of V5, FLAG and background nearby for each band was measured using ImageJ v1.53. To obtain the corrected integrated density, the background value for each band was subtracted. The V5/FLAG ratio was then calculated using the corrected integrated densities and normalized to the highest signal detected for FLAG.

Figure 5 Fibroblasts from individuals with TRAPPC6B variants display membrane trafficking defects and have fragmented Golgi. A. Fibroblasts from families 4 (c.149+2 T>A splice-site; Patients 5 and 6) and 15 (p.Q152*; Patients 23 and 24) were transfected with ST-GFP and incubated overnight. The next day, cells were treated with 60 µM biotin and imaged every 2 minutes. Golgi-associated fluorescence was quantified and plotted as a function of time. In some cases, TRAPPC6B-RFP was co-transfected to verify a rescue of the trafficking defect. The error bars represent the SEM (standard error of the mean) at each time point. **B.** Representative images used for quantification of the RUSH trafficking assay at 0, 10, 20 and 30 minutes. N values ranged from 48-61 and come from at least three biological replicates. The scale bar represents 10 µm. **C.** Fibroblasts were either un-transfected or transfected with TRAPPC6B-RFP, fixed and stained for mannosidase II as a Golgi marker. The mannosidase II-positive structures were quantified as described in the methods section. Bars represent SEM. N values ranged from 65-82 and come from at least three biological replicates. **D.** Representative images used for the quantifying the number of Golgi fragments. The scale bar represents 10 µm.

Figure 6 Neuronal TRAPPC6B knockdown impairments in a *Drosophila* model. A. Box and whisker plot of distance traveled in 3 seconds in negative geotaxis assay comparing Gal4 and UAS driver heterozygotes and shRNA neuronal-driven expression for TRAPPC6B knockdown. Statistics determined using paired t-test (n=16 trials). Boxes represent 25th and 75th percentiles with median line; whiskers represent range of data.* $p<0.01$, ** $p<0.001$. **B.** Erect wing phenotype is significantly increased in TRAPPC6B knockdown compared to heterozygous

controls. (n=113-137 flies/genotype). Statistics determined both as a 3-way and pairwise against individual controls using Chi-squared analysis. * p<0.01.

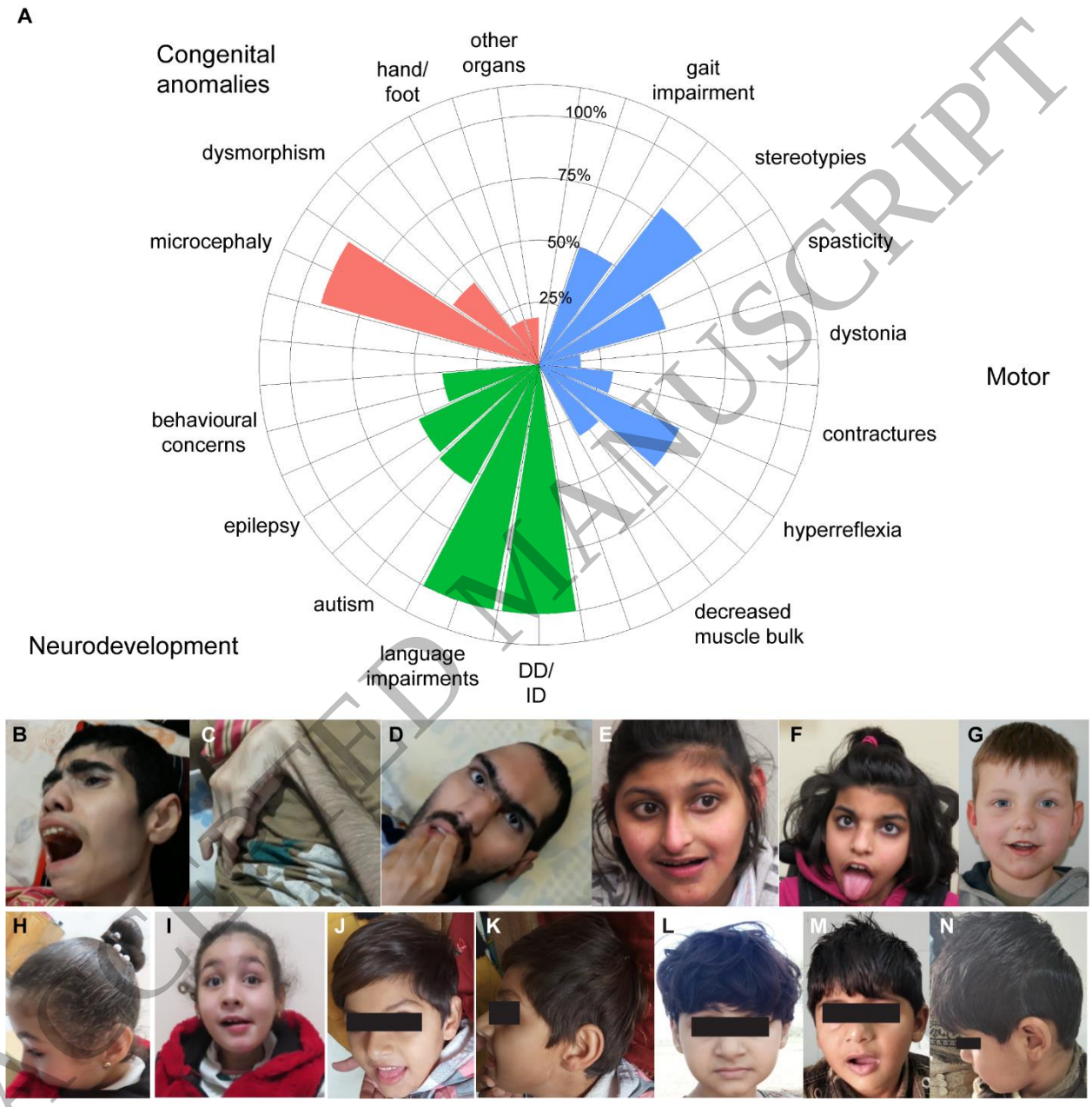

Figure 1
165x166 mm (x DPI)

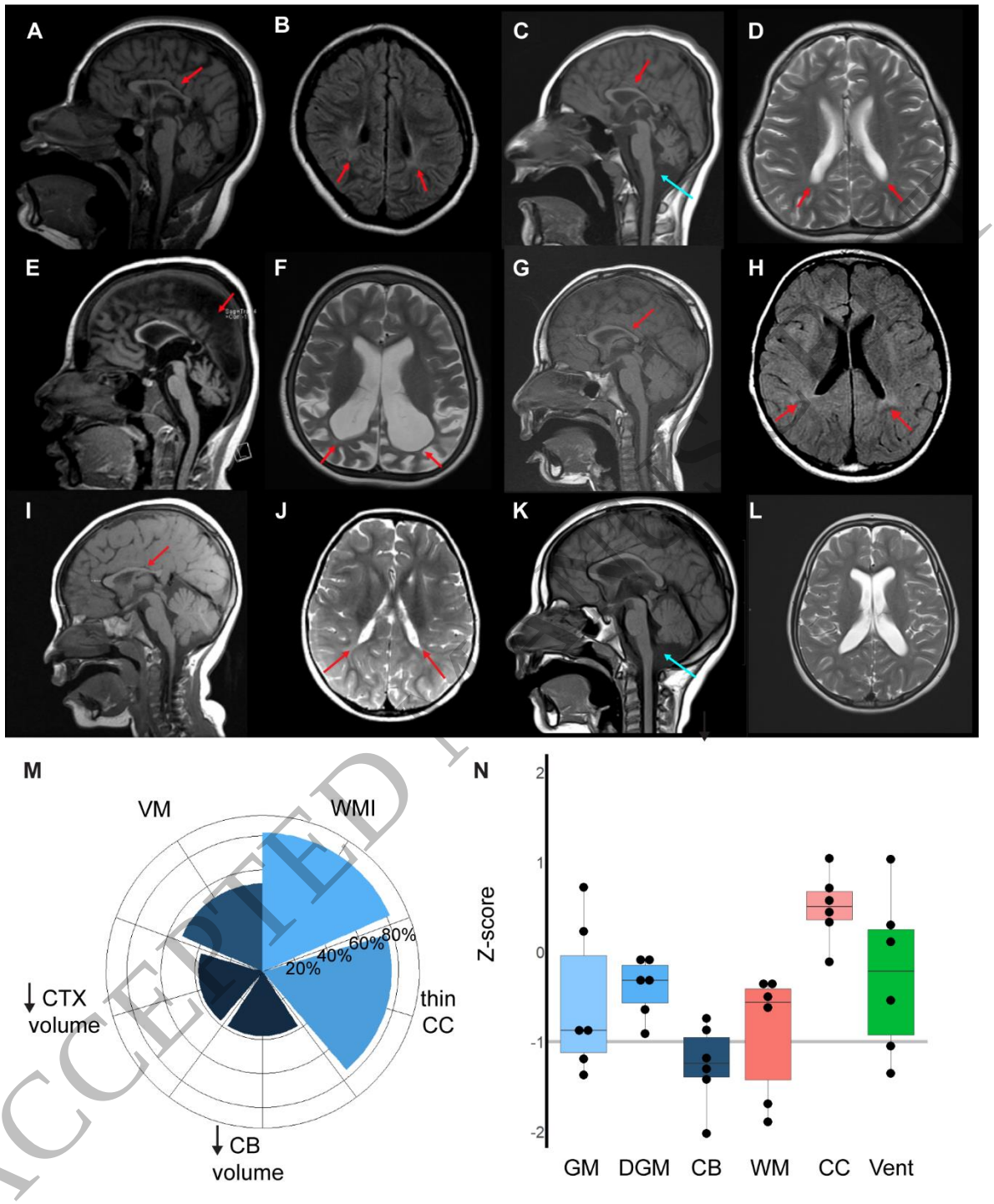

Figure 2
154x187 mm (x DPI)

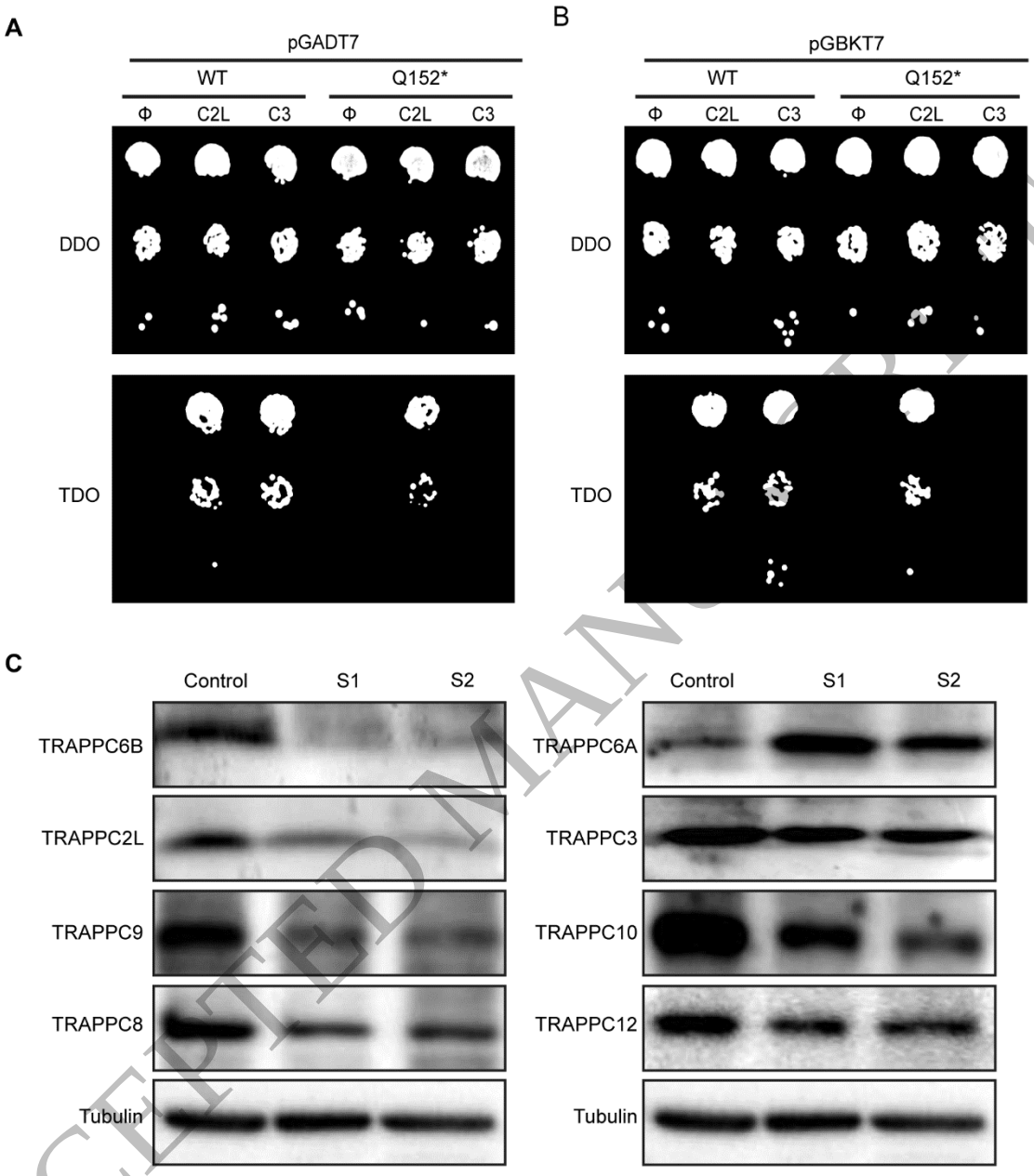

Figure 3
146x169 mm (x DPI)

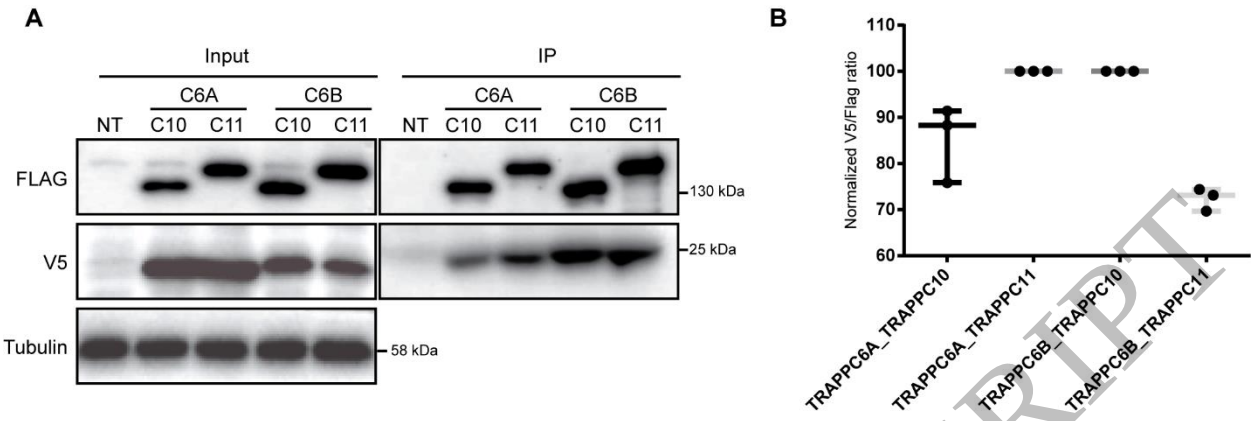

Figure 4
165x55 mm (x DPI)

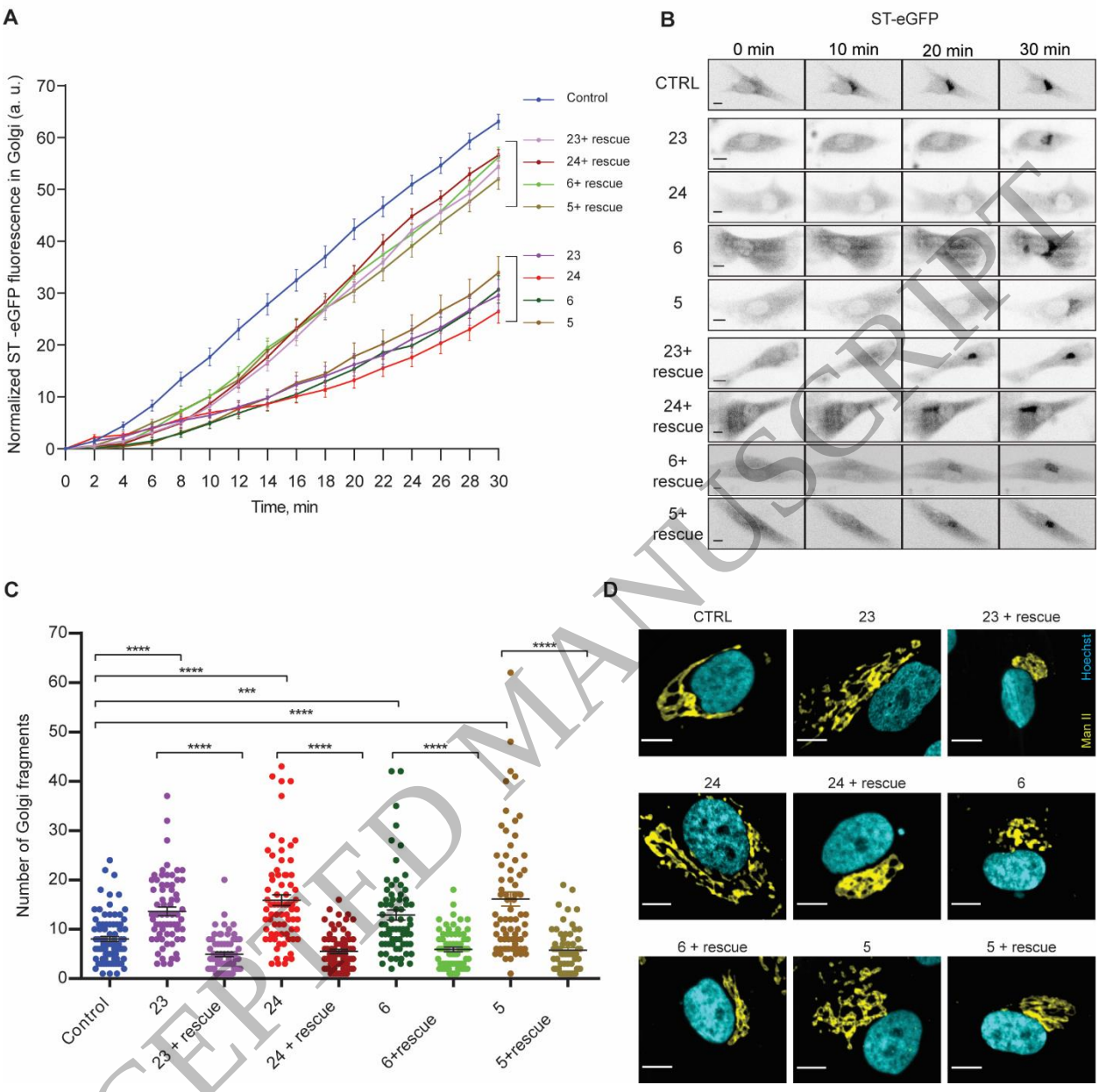

Figure 5
165x163 mm (x DPI)

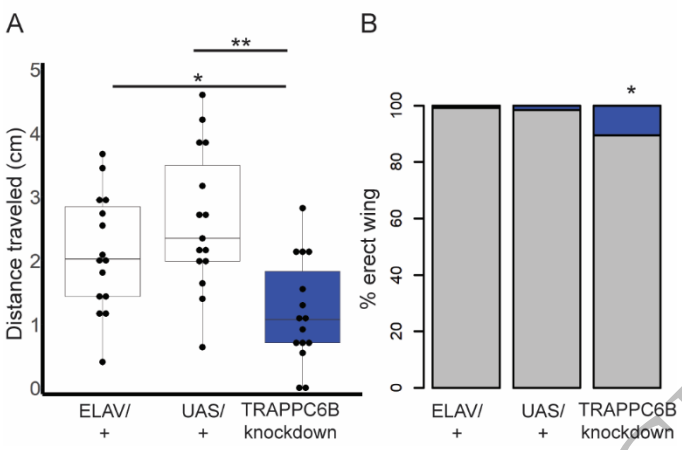

Figure 6
89x59 mm (x DPI)

1

2 **Table 1 TRAPP genes with neurological disease connections**

Gene (OMIM#/*), citation	Complex	Disease	Cognitive findings	Epilepsy	Movement disorder	White matter	Brain volume	Language	Dysmorphic features	Visual system	Muscle findings
TRAPPC6B (#617862), this study	II, III	NEDMEBA	ID	Variable	Spasticity, dystonia, stereotypies	Thin corpus callosum, hyperintensity	Brain volume loss, microcephaly	Absent expressive language	Variable	No impairments	Reduced bulk
TRAPPC2L (#618331)[12,31]	II, III	PEERB	ID	Focal seizures and status epilepticus with infection	Tetraplegia; dystonia	Normal-delayed myelination	Variable atrophy	Absent speech	NR	Cerebral visual impairment	Rhabdomyolysis; Nonspecific biopsy
TRAPPC4 (#618741)[15,32,33]	II, III	NEDESBA	Normal-severe ID; regression	Yes	Spasticity; axial hypotonia; variable dyskinesia	White matter loss	Mild-severe cerebral atrophy; secondary microcephaly	Delay and loss of expressive language	Yes	Visual impairments; variable cataracts	Amyotrophy
TRAPPC6A (*610396)[34]	II, III	NDD	ID	NR	NR	NR	NR	Speech delay	Yes	NR	NR
TRAPPC9 (#613192)[35,36]	II	MRT13	Moderate-severe ID	Variable seizures	Hypotonia, stereotypies	Thin corpus callosum, reduced white matter	Postnatal microcephaly	Speech disorder	Yes	NR	NR
TRAPPC10 (*602103)[24,37]	II	NDD	Severe ID	Variable seizures	Hypotonia, waddling gait	1 patient thin corpus callosum	Microcephaly	Poor speech	NR	Low frequency strabismus	NR
TRAPPC11 (#615356)	III	LGMD	Normal-	Variable (general	Some with	Some reduced	Normal-microcep	NR	NR	Variable (amblyo	Limb girdle muscular

[38]			severe ID	ized seizures)	ataxia and/or choreiform movements	volume	haly; some cerebral atrophy			pia, cataract)	dystrophy
TRAPPC12 (#617669) [39]	III	PEBAS	Severe DD and regression	Seizures; myoclonus	Spasticity; truncal hypotonia; dystonia	Corpus callosum agenesis; hyper-intensity	Microcephaly; pons hypoplasia; diffuse atrophy	NR	NR	Optic atrophy; cortical visual impairment	NR

ID = intellectual disability; LGMD = limb girdle muscular dystrophy; MRT13 = mental retardation, autosomal recessive 13; NDD = neurodevelopmental disorder; NEDESBA = Neurodevelopmental disorder with epilepsy, spasticity, and brain atrophy; NEDMEBA = neurodevelopmental disorder with microcephaly, epilepsy, and brain atrophy; NR = not reported; PEBAS = progressive encephalopathy with brain atrophy and spasticity; PEERB progressive encephalopathy with episodic rhabdomyolysis. # = phenotype MIM number, * = gene/locus MIM number.

Table 2 Clinical features of TRAPPC6B patients

Family	Patient	Walk	Sit	GMFCS	Verbal	Seiz.	Spast.	Contractures	Dystonia	Reflex	Muscle loss	Stereotypies	Microcephaly	Facial feat.	Hand/foot	Other organ	ID/GDD	ASD	Behavioral
1	1	++	++	5	+	+	+	+	+	-	+	+	Yes	+	0	0	+	0	0
	2	++	++	5	+	+	+	+	+	0	+	+	Yes	+	0	0	+	0	0
2	3	++	+	5	+	+	++	+	0	+	N/A	+	Yes, prog.	+	+	0	+	N/A	0
3	4	+	0	N/A	+	+	++	+	+	N/A	N/A	+	−3 SD 35y	+	+	0	+	N/A	+
4	5	+	0	4	+	++	0	0	0	+	+	+	−6.5 SD 15y	+	+	0	+	N/A	0
	6	++	+	5	+	0	0	+	0	+	+	+	−6 SD 11y	+	+	+	+	N/A	0
5	7	0	0	3	+	0	0	0	0	0	N/A	+	No, −1.3 SD 3.5y	+	0	+	+	0	+
6	8	0	0	2	+	0	0	0	0	0	N/A	+	−2.5 SD 5y	+	+	+	+	0	0
7	9	0	0	N/A	+	0	+	0	0	0	+	+	−2 SD birth	+	0	0	+	N/A	0
8	10	+	0	N/A	+	+	Yes	0	0	+	N/A	+	−2 SD birth	+	+	0	+	+	+
9	11	0	0	N/A	+	0	0	0	0	0	N/A	+	−2 SD 4y4m	0	0	+	+	+	+
	12	0	0	N/A	N/A	0	0	0	0	0	N/A	N/A	−2 SD	0	0	0	+	+	+
10	13	0	0	N/A	+	++	0	0	0	N/A	N/A	N/A	−5.2 SD 11y	+	0	0	+	+	0
	14	0	0	N/A	+	0	0	0	0	N/A	N/A	N/A	−5.7 SD 6y	0	0	0	+	+	0
	15	++	0	N/A	+	0	0	0	0	N/A	N/A	N/A	−2.4 SD 14m	0	0	0	+	+	0
	16	0	0	N/A	+	0	0	0	0	N/A	N/A	N/A	N/A	0	0	0	+	0	0
11	17	++	0	N/A	+	0	Yes	+	0	0	N/A	+	N/A	0	0	0	+	N/A	0
	18	0	0	N/A	+	0	0	+	0	0	N/A	+	Yes	0	0	0	+	N/A	0
12	19	0	0	N/A	+	++	Yes	0	0	0	N/A	N/A	Yes	0	0	0	+	+	0
	20	+	0	N/A	+	0	0	0	0	0	N/A	0	Yes	0	0	0	+	N/A	0

13	21	++	0	4	N/A	++	++	N/A	0	N/A	N/A	+	−2 SD birth	+	+	0	+	+	0
14	22	0	0	N/A	N/A	++	Yes	+	0	+	N/A	+	−4.3 SD 5y	0	0	0	+	+	0
15	23	0	0	N/A	+	0	0	0	0	+	N/A	+	No −1.4 SD	0	0	0	+	+	+
	24	0	0	N/A	+	0	0	0	0	+	N/A	0	No −0.5 SD	0	0	+	+	0	0
16	25	0	0	N/A	+	0	+	+	+	+	0	+	−4.8 SD	+	0	+	+	+	+
	26	0	0	N/A	+	0	+	+	+	+	0	+	−4.8 SD	+	0	+	+	+	+
17	27	0	0	N/A	+	++	+	N/A	0	N/A	0	0	−2.4SD 30y	0	0	0	+	0	0
	28	0	0	N/A	+	++	+	N/A	0	N/A	0	0	−2.8 SD 30y	0	0	0	+	0	0
18	29	+	0	4	+	++	+	0	0	+	N/A	0	Yes, 46 cm	0	0	0	+	0	0

Symbols describing features: + defects present; 0=no abnormalities; N/A data not available. Facial features include bitemporal narrowing, narrow nasal bridge, deep/wide-set eyes. Hand or foot features include syndactyly, tapered, thin, or hypoplastic digits, and arachnodactyly affecting either the hands and/or feet. Other organs include cardiac, genito-urinary, liver, and eye. Behavioral concerns include anxiety, self-injury, hyperactivity, and aggression. Walking (0=walks unassisted, += walks with assistance or gait impairment present, ++=cannot walk) Sitting (0=sits without support, +=sit with support, ++=cannot sit); Verbal (0=normal speech, +=impaired age-appropriate expressive language); Seiz. (0=no seizures, +=only 1 seizure in medical history, ++=epilepsy); Spasticity (0=none, +=lower limbs only,++=upper+lower body involvement); Dystonia (0=no, +=generalized affecting ≥2 limbs); Reflex (-=absent knee-jerk reflex, 0=normal, +=exaggerated/brisk) Muscle loss (0= none, +=atrophy or reduced bulk with or without hypotonia) Autism (0=no, +=yes. N/A may also refer to inability to assess due to ID severity).